Pole-Placement Self-Tuning Control of a Fixed-Bed Autothermal Reactor

Part I: Single Variable Control

A pole-placement self-tuning controller has been used to control a fixed-bed autothermal reactor conducting the water-gas shift reaction at both an upper stable state and a middle unstable state. Excellent set-point tracking and disturbance rejection characteristics were obtained using a single manipulated variable, the heat input at the entrance to the catalyst bed, to control a single bed temperature. Excellent set-point tracking during the transition from the upper state to the middle state was obtained by using a technique that tuned the closed-loop poles on-line so as to give an optimal response.

P. E. McDermott, D. A. Mellichamp, R. G. Rinker
Department of Chemical and Nuclear Engineering
University of California
Santa Barbara, CA 93106

SCOPE

The control of fixed-bed reactors has received considerable interest in recent years due to its importance to the chemical process industry. Several single- and multivariable control approaches have been successfully applied to a variety of reaction systems (Bonvin et al., 1983a, b, c; Clement et al., 1980; Foss et al., 1980; Harris et al., 1980; Jutan et al., 1977a, b, c, d, 1980; Silva et al., 1979; Sorensen et al., 1976, 1977, 1980; Tremblay and Wright, 1977; Wallman et al., 1979; Wong et al., 1983; Wright et al., 1977). The controller design methodology employed in these studies has involved one of two approaches:

1. The phenomenological modeling of the reactor followed by model reduction to obtain a low-order model required for control design, or
2. Off-line analysis of input-output disturbance data to identify the low-order model.

The first method of controller design is very time-consuming and potentially very costly. Both of these methods suffer from the disadvantage that the resulting controller is only valid around the steady state at which it was designed. Consequently, if reactor conditions (e.g., catalyst activity, heat inputs, feed flow rate or composition) change with time, the controller will no longer be valid.

The idea of identifying a model of the process on-line and adjusting the controller parameters based on this model, referred to as self-tuning control, was first proposed by Kalman (1958). However, interest in self-tuning control did not really begin until the development of the self-tuning regulator (STR) by Åström et al. (1973, 1974, 1977) for single-input/single-output systems. Several shortcomings of the STR led to the development of the self-tuning controller (STC) by Clarke and Gawthrop (1975, 1979, 1981), the pole-placement controllers of Wellstead et al. (1979a, b, c, 1981) as well as Åström and Wittenmark (1980), and other algorithms (Vogel, 1982; Vogel and Edgar, 1982; Allidina and Hughes, 1980; McDermott and Mellichamp, 1984a).

Self-tuning controllers have several advantages compared to the above methods of controller design. Self-tuning controllers are easy to implement and are applicable to processes with a wide variety of characteristics—unknown parameters, the presence of time-delay, time-varying process dynamics, and stochastic disturbances. These advantages explain why self-tuning controllers have been successfully applied to many chemical processes. The recent review paper by Se-

Correspondence concerning this paper should be addressed to R. G. Rinker.

borg et al. (1983) lists the major applications of self-tuners. In the area of reactor control, several numerical and experimental studies have been performed. Hodgson and Clarke (1982) have considered the application of the STC to batch reactors. Åström (1978) studied the pole placement control of a seventh-order linear model of a fixed-bed reactor. Harris et al. (1980) considered the self-tuning control of a laboratory-scale butane hydrogenolysis reactor. McDermott and Mellichamp (1984b) investigated the pole-placement self-tuning control of a 36th-order nonlinear fixed-bed autothermal reactor model operating at an unstable state. Lee and Lee (1985) used a self-tuning regulator to control the temperature in a butane oxidation reactor.

In this paper, single-input/single-output self-tuning control of a fixed-bed autothermal reactor is considered. (In Part II, we consider multiinput/multioutput self-tuning control of the reactor.) The pole-placement self-tuning controller (McDermott and Mellichamp, 1984a) is used to control a single temperature in the catalyst bed immediately before the hot spot. Control at both an upper stable state and an unstable state, as well as the transition between the two states, is demonstrated.

CONCLUSIONS AND SIGNIFICANCE

The pole-placement self-tuning controller of McDermott and Mellichamp (1984a) has been used to control a fixed-bed autothermal reactor. With only a single temperature measurement, a catalyst bed temperature immediately before the hot spot, excellent set point responses and disturbance rejection characteristics to stochastic and large steplike deterministic disturbances were obtained by manipulating the heat input at the entrance to the catalyst bed. The controller performed equally well at both an upper stable state and at an unstable state, indicating that the adaptation techniques were very robust. The use of very low-order models for the controller design also indicates the excellent robustness characteristics of the controller. On-line self-tuning of the controller poles yields excellent system response properties over a wide range of operating conditions, in particular during transitions from the upper stable steady state to the unstable state. These features enable the self-tuning controller to match the large spectrum of properties exhibited by this highly nonlinear process.

Experimental Autothermal Reactor System

Reactor facility

The reactor facility used in this study is a modified version of one used in previous studies (Ampaya and Rinker, 1977, 1978; Lee 1978; Wong et al., 1983). It consists of a thermally insulated fixed-bed reactor with internal countercurrent heat exchange for conducting autothermally catalyzed exothermic reactions. The reactor is fully instrumented to measure temperatures, flow rates, energy inputs, and inlet and exit compositions. These measurements have been automated using on-line digital processing equipment interfaced to the department computer facility described in the next section.

A flow diagram of the reactor system is given in Figure 1. Gaseous feed components (CO, CO_2, and H_2), supplied from pressure-regulated cylinders, flow individually through computer-controlled mass flowmeters/flow-controllers (Union Carbide model FM-4550). The individual gas streams are then mixed and passed through a temperature-controlled sparger (100°C) that saturates the mixture with water. The water level in the sparger is automatically controlled to ensure saturation of the gas mixture. The wet gas is preheated to approximately 500°C in a Lindberg furnace before entering the reactor. All lines between the sparger and the furnace, and between the furnace and the reactor are heated and thermally insulated.

The feed gas enters the reactor at the bottom and flows radially inward, between two circular Macor plates. A porous metal diffuser causes the gases to flow tangentially around the plates, before flowing inward, to ensure uniform flow in the annulus. The gas then flows past a final preheater before entering the annulus.

The cylindrical outer wall of the reactor is constructed from a machinable ceramic (Macor) that has a low thermal conductivity and heat capacity, and represents a significant barrier to heat loss. A schematic diagram of the reactor is shown in Figure 2 and the dimensions of the reactor are given in Table 1. The inner concentric tube is made of stainless steel (type 316) and contains the water-gas shift catalyst (Girdler G-3). Heaters are wrapped on the Macor outer surface to facilitate start-up and to compensate for heat losses. The reactor is covered with a 6 in (15 cm) layer of Kaowool insulation.

Product gases leave the reactor at the bottom of the catalyst bed and flow through an inert packed bed to minimize end effects. The hot product gas is cooled using a tapwater-cooled multitube heat exchanger. Most of the excess water is condensed in the heat exchanger. The cooled product gas then is fed to a wet-test meter for final flow measurement.

Compositions of all feed and product streams are measured with a Hewlett-Packard model 5830A gas chromatograph using 4-ft (1.2 m) columns containing Carbosieve B. Species separation is achieved using temperature programming (70°C for 2.2 min, 30°C/min increase for 1.33 min, and 110°C for 2 min). The output signals from the thermal conductivity detector are integrated and reported by the H-P model 5930A electronic integrator.

Temperatures in the outer wall and in the catalyst bed are measured with chromel-alumel thermocouples. The thermocouples in the catalyst bed enter at the bottom of the reactor and are

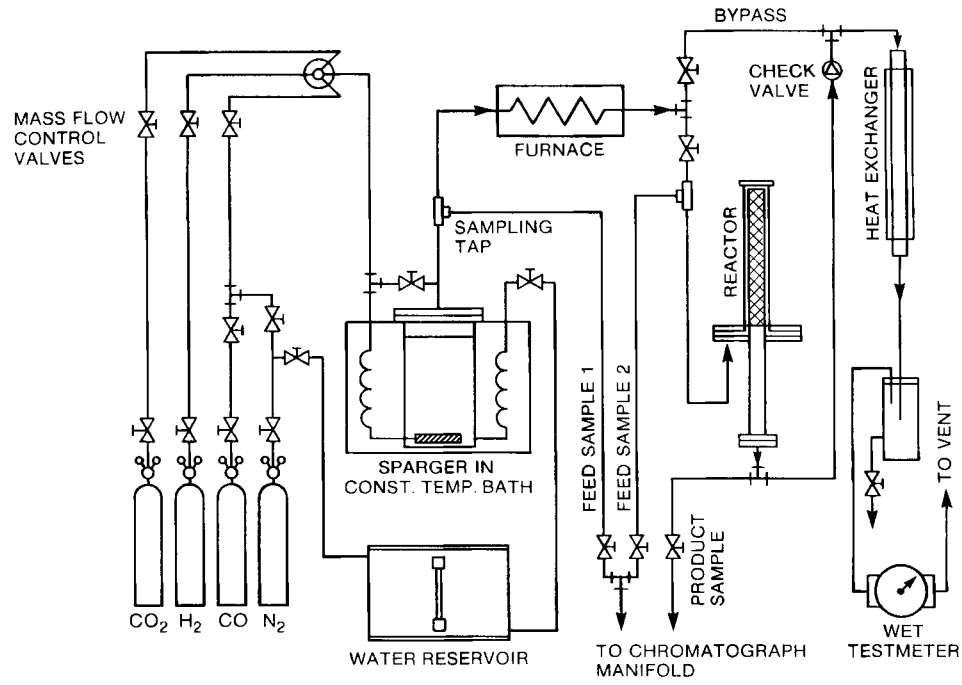

Figure 1. Flow diagram of autothermal reactor with internal countercurrent heat exchange (ARICHE) facility using water-gas shift reaction.

positioned axially at seven measurement points (Table 2 gives the locations of the thermocouples). These points correspond to collocation points used in the modeling studies (McDermott 1984). Their dimensionless radial position is at 0.707, which corresponds to the mean bed temperature at each axial location.

Three instruments are connected in parallel to monitor the thermocouple voltages: a Monitor Lab model 9400 scanner, a Leeds and Northrup Type K3 potentiometer, and an Esterline-Angus model 1124E multipoint potentiometric recorder. The scanner is capable of reading the entire array of thermocouples and transmitting the data to the computer in approximately 20 s. Since the transit time of a thermal wave through the catalyst bed was found to be approximately 6 min, the scanner is quite adequate for monitoring transient responses in the bed.

Two heaters in the reactor allow for computer control of the system. A small 20 W heater at the top of the reactor (the turnaround point) directly affects the temperature of the feed gas entering the catalyst bed. A larger 60 W heater located at the inlet of the reactor allows for direct manipulation of the feed temperature.

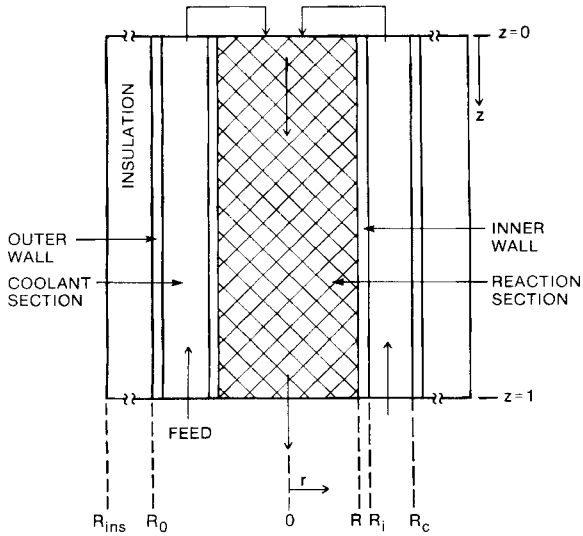

Figure 2. Diagram of ARICHE.

Data logging and computer control facility

A block diagram of the computer control facility is shown in Figure 3. The scanner receives signals from reactor thermocouples, from the two heaters, and from the mass flowmeters. The signals are converted to digital representation and transmitted via a cable to a nearby laboratory housing a Data General Eclipse S-130 computer for on-line data processing. The scanner has been modified to provide the interface for computer operation of the feed heater, top heater, and mass flow-controllers. In this case, digital signals from the computer are converted to analog voltages for driving the regulated power supplies or for driving the flow-controllers.

Table 1. Physical Dimensions of the Macor Reactor

Reactor length, m	20.32×10^{-2}
Inside dia. of inner tube, m	2.36×10^{-2}
Outside dia. of inner tube, m	2.54×10^{-2}
Inside dia. of outer tube, m	2.84×10^{-2}
Outside dia. of outer tube, m	4.31×10^{-2}
Dia. of insulation, m	23.0×10^{-2}
Catalyst particle dia., m	1.0×10^{-3}

Table 2. Thermocouple Locations, Dimensionless Distance from Top of Catalyst Bed

Outer Wall	Catalyst Bed
0.0	—
	0.048
	0.115
	0.206
	0.316
	0.437
0.5	—
	0.563
	0.794
	0.991
1.0	—

Experimental Procedure

Start-up and operation of the reactor was similar to that used in previous studies (Ampaya and Rinker, 1977, 1978; Wong et al., 1983) with several modifications required because of changes in the reactor. The reactor was first purged and heated to approximately 100°C with dry nitrogen, and then to approximately 225°C with wet nitrogen. During this time, the two control heaters along with a heater on the reactor outer wall were all increased at the following rates: feed heater = 5 W/h; turnaround heater = 1 W/h; reactor heater = 5 W/h.

When the maximum temperature in the reactor reached 225°C, wet-process gas containing only CO and H_2 was switched on in order to condition the catalyst. During this start-up period, heating continued at a rate of approximately 50°C per hour. Higher rates were avoided to prevent damage to the Macor walls and to the catalyst, and to allow sufficient time for conditioning. This procedure helped to ensure that the activity of the catalyst remained the same for all experiments. When the bed temperatures reached approximately 425°C, process gas with the reaction mixture was introduced (Table 3 gives the final steady state operating conditions).

As the temperatures in the reactor approached the desired operating temperatures, the heater on the outer wall was decreased at a rate of 5 W every 15 min until it was off. At this time, a small 10 W heater above the reactor inside the insulation was turned on to compensate for heat losses at the top of the reactor.

After the temperatures in the catalyst bed reached steady state values, final adjustments were made to the turnaround and feed heaters. These heaters were set to 10 and 40 W, respectively, to allow for manipulation in both positive and negative directions. The top compensation heater was then adjusted to keep heat losses to a minimum.

Shut-down was accomplished by turning off the process gas and switching to dry nitrogen. A flow rate of 1 L/min allowed the reactor to cool down to ambient conditions overnight.

Controller Design and Implementation

Controller design

The controller used in this study is an extension of the self-tuning controller (Clarke and Gawthrop, 1975) made by McDermott and Mellichamp (1984a) that includes variable dead-time compensation and autotuning of the desired closed-loop poles. A short description of the controller is given here. The complete derivation can be found elsewhere (McDermott, 1984).

Like most fixed-bed reactors, the autothermal reactor exhibits a so-called inverse (or wrong way) response for changes in the heat input. The original self-tuning controller was designed to handle these types of processes. However, when the reactor is operating at the unstable state, the only way closed-loop stability can be guaranteed is to use a pole-placement controller.

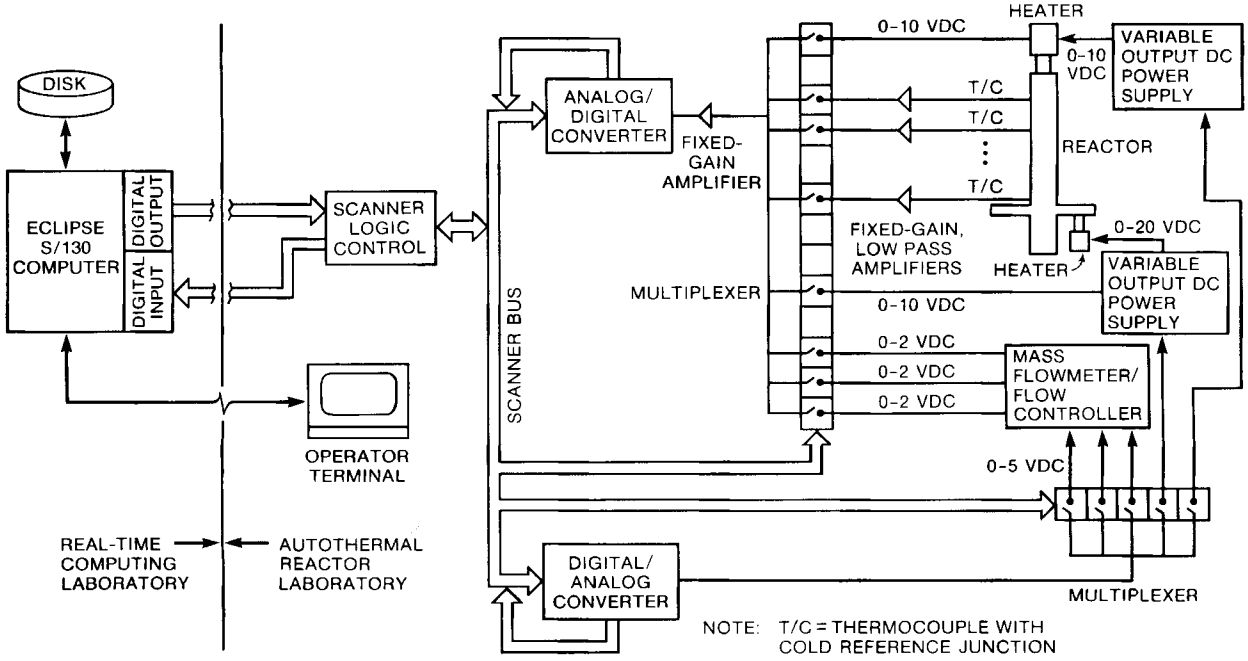

Figure 3. Diagram of control hardware and interface with real-time computer.

Table 3. Operating Conditions

Inlet pressure, MPa	0.166
Pressure drop across bed, MPa	0.051
Feed rate, kg/s	2.19×10^{-4}
Feed temperature, K	655
Ambient temperature, K	298
Feed composition CO, mol%	13.7
Feed composition H_2O, mol%	52.1
Feed composition CO_2, mol%	22.2

The pole-placement controller used in this study is designed to work with processes described by single-input/single-output, linear, discrete-time, randomly-disturbed models

$$A(z^{-1})y(t) = z^{-k_{min}}B(z^{-1})u(t) + C(z^{-1})\xi(t) + d \qquad (1)$$

where $u(t)$ and $y(t)$ are the deviations from the mean of the system's input and output, respectively; $A(z^{-1})$, $B(z^{-1})$, and $C(z^{-1})$ are polynomials in z^{-1} of orders n_A, n_B, and n_C, respectively, with a_0 and $c_0 = 1$; d is a constant offset; k_{min} is the minimum expected process dead time; and ξ is an uncorrelated random sequence of zero mean. Obviously, the linearity requirements are met with the autothermal reactor only in the vicinity of the operating point.

The control law is determined so as to minimize the variance of the generalized output, $\phi(t + k_{min})$,

$$I = \min \epsilon[\phi^2(t + k_{min})] \qquad (2)$$

where $\epsilon[\cdot]$ is the expectation operator. $\phi(t + k_{min})$ is chosen to be

$$\phi(t + k_{min}) = P(z^{-1})y(t + k_{min}) + Q(z^{-1})u(t) - R(z^{-1})y_r(t) \qquad (3)$$

where $P(z^{-1})$, $Q(z^{-1})$, and $R(z^{-1})$ are arbitrary polynomials in z^{-1}, and $y_r(t)$ is the set point at time t. Equation 3 cannot be used directly in the objective function, I, since unknown future data points are required. However, a k_{min} step-ahead predictor of $\phi(t + k_{min})$ can be derived to obtain the control law

$$u(t) = -\frac{Fy(t) - Hy_r(t) + \gamma}{(CQ + BE)} \qquad (4)$$

where E and F are polynomials in z^{-1}; $H = CR$, and $\gamma = E(z^{-1} = 1)d$.

Applying the control given by Eq. 4 to the process model Eq. 1 yields the following closed-loop behavior

$$y(t + k_{min}) = \frac{BR\,y_r(t)}{PB + QA} + \frac{BE + CQ}{PB + QA}\xi(t + k_{min}) + \frac{(BE + CQ)d - B\gamma}{(PB + QA)C} \qquad (5)$$

The pole-placement approach is to choose P and Q such that the closed-loop poles are at prespecified locations

$$PB + QA = V \qquad (6)$$

where V is a polynomial in z^{-1}. The roots of $V(z)$ are the desired values of the poles inside the unit circle. Details of how these roots are obtained are given by McDermott (1984).

The pole-placement controller given by Eq. 4 will have integral action whenever a good estimate of the offset parameter, d, is available. However, during periods of upset, an estimate of d is not available. The procedure outlined by McDermott and Mellichamp (1984a) where an extra integrator is inserted into the loop should be used when an estimate of d is not available. The resulting control law then becomes

$$u(t) = -\frac{F^{\dagger}y(t) - Hy_r(t)}{(CQ + BE^{\dagger})} \qquad (7)$$

The d term does not appear in this form of the control law, so it is advantageous to use Eq. 7 whenever an estimate of d is unavailable. It is also important to note that the denominator polynomial, $CQ + BE^{\dagger}$, now has a pole at $z = 1$, so the controller will have integral action.

The autotuning algorithm was developed by McDermott and Mellichamp (1984a) to enable a single nonzero closed-loop pole to be positioned on-line so as to optimize the set point response. The unweighted objective function for the optimization takes the form

$$I = \sum_{j=1}^{N} [y(j + k_{min}) - y_r(j)]^2 \qquad (8)$$

where y is available from the closed-loop expression

$$y(t) = \frac{BR}{V}y_r(t) \qquad (9)$$

In many cases, a single nonzero closed-loop pole is sufficient to give excellent closed-loop response characteristics; thus, $V(z^{-1})$ becomes

$$V(z^{-1}) = 1 - v_1 z^{-1} \qquad (10)$$

The result of this choice is to require the system to respond as a first-order system, with time constant equal to $-T_s/\ln(v_1)$, where T_s is the sampling period and v_1 is the nonzero z-domain closed-loop pole.

The coefficients of R are chosen such that Eq. 5 has a unity gain for $y_r(t)$. Thus, during periods when the process model (more specifically B) is changing, the coefficients of R must also change. McDermott and Mellichamp (1984b) have shown that for pole-placement controllers, the closed-loop pole should also be retuned whenever the process changes in order to achieve the optimal performance of the controller. Since the coefficients of R give an indication when the process has changed, any one of the coefficients can be used to reinitiate the autotuning of the pole. Practically speaking, whenever r_i (where $i = 0, 1, \ldots, n_R$) changes by a certain amount, for example $\pm 5\%$, the controller can be instructed to autotune the poles.

Control implementation

For purposes of observing the reactor behavior in detail, all eight catalyst bed temperatures, along with the feed temperature and the temperature at the turnaround point were measured at each sampling instant. The single controlled tempera-

ture utilized an average of three thermocouple readings so as to reduce the high-frequency noise characteristics of the data logging system and reactor. Although the controller derivation assumes that these measurements are taken at the same point in time, the approximately 20 s required to measure all the temperatures, heat inputs, and mass flow rates is quite fast in comparison to the reactor dynamics.

The parameters of the process model, $A(z^{-1})$, $B(z^{-1})$, $C(z^{-1})$, and d were identified using recursive extended least-squares with upper-diagonal factorization of the covariance matrix ($\underline{P}$). A pseudorandom binary (PRB) signal was added to the controller output so as to excite the process during the initial stages of the identification. The amplitude of the PRB signal was calculated as a linear function of the trace of the parameter covariance matrix. (The maximum amplitude of the PRB signal was 0.5 W when the trace had a value of 5.) Hence, as the parameters converged and the trace became small, the PRB signal became small.

During normal operation of the pole-placement controller, control was calculated using Eq. 4. At each time step, a decision was made to determine if $P(z^{-1})$ and $Q(z^{-1})$ should be recalculated. If the absolute value of the residual, $y_{\text{actual}} - y_{\text{estimated}}$, was less than σ, the standard deviation of the noise, then the estimated model was assumed to be a good representation of the process. In this case, the previous values of P and Q were used. The polynomial identity was resolved at each time step to account for slight variations in the estimated parameters.

Whenever the estimation error exceeded σ, the system of simultaneous linear equations, Eq. 6, had to be solved on-line. However, if $A(z^{-1})$ and $B(z^{-1})$ have a common root, the system is indeterminant. To ensure that this did not happen during any of the control runs, several checks were included in the control program:

1. Whenever the determinant of the system of equations was found to be below a certain threshold (chosen to be 0.001), the previous P and Q polynomial coefficients were used.

2. Whenever the calculated p_0 (the leading coefficient in the P polynomial) changed by more than $\pm$ 1, the previous P and Q coefficients were again used.

If the absolute value of the residual exceeded the noise level of the process, assumed to be 10σ, the estimated model no longer could be taken as a good representation of the process. This usually happened after a load disturbance entered the reactor. Covariance resetting, i.e., the addition of a constant diagonal matrix to the covariance matrix, caused a new model to be reidentified (a factor of 100 $\underline{I}$ was used in all the runs). However, during this period of reestimation, the parameters varied significantly, and control based on these inaccurate parameters could have caused the closed-loop system to go unstable. Hence, during this period, the most recent previous estimates of the parameters, i.e., those used before the estimation was restarted, were used in the control law given by Eq. 7. Since this controller was based on the old process model, an exponential filter prevented the controller from taking too vigorous control action. The new model was assumed to have converged when the value of the trace had again dropped below 15.

Results and Discussion

In all of the runs, the temperature measurement location was chosen to be at $z = 0.206$ (dimensionless distance from the top of the reactor), and the manipulated variable was taken to be the heat input at the entrance to the catalyst bed. The sampling period chosen for the first three sets of runs was 40 s and $k_{\min}$ was chosen to be 1. The orders of A, B, and C were 1, 3, and 1, respectively. Eigenvalue and structural dominance analysis of the linear model of the reactor (McDermott, 1984) has shown that the system is dominantly first-order. Thus the choice of unity for n_A is reasonable. In any case, a higher order B polynomial can account for more complex behavior, such as inverse response characteristics. In order to deal with expected changes in the process model, the following techniques were employed: the variable forgetting factor (Fortiscue and Kershenbaum, 1981) with sigma $\Sigma_0 = 100$, the fault detection method of Hägglund (1982), and the covariance resetting discussed above. Autotuning of the closed-loop pole was initiated whenever r_o changed by +5 or −10%.

Control at the upper stable steady state

Figure 4 shows the response of the reactor to step changes in the set point and the load variable, feed flow rate. Since the closed-loop pole has been tuned to give an optimal set point response, the response of the reactor to the change in the set point is very good, with the exception that there is a slight overshoot for the initial change in the set point. This characteristic is a result of the system nonlinearities that are important when such a large amount of control action is used. At t equals 3 h, the flow rate of dry feed gases was decreased by 20%. The controller at first overcompensates by taking too much control action, but it is soon able to bring the reactor back to the set point. Note that a 20% change in the reactor feed flow rate represents a

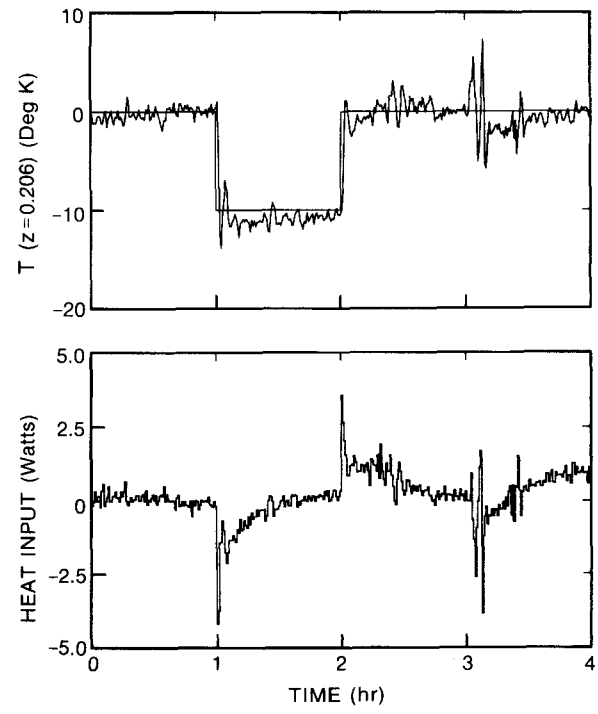

Figure 4. Response of reactor to set point and load (feed flow rate) step changes at upper stable steady state.

drastic disturbance, i.e., one that results in a radical change in the dynamic characteristics of the process.

Figure 5 shows that there is a jump in the residual when the set point is changed. This characteristic indicates again that the nonlinearities are important for this amount of change in the control action. The big jump in the residual at $t = 3$ h is due to the load change. The behavior of the trace of the covariance matrix is also shown in Figure 5. The small jumps result from the operation of the fault detection method, and indicate that the estimated model must continually change as the system nonlinearities become important. The large change at $t = 3$ h is due to the covariance resetting.

The behavior of the model parameters during this run is shown in Figure 6. The a_1 parameter is relatively constant until the load disturbance occurs. Since covariance resetting has been initiated at this point, a large change in the parameter is expected. The parameter then settles out a short time after the load change. The B parameters wander around much more than the a_1 parameter since they effectively must model the changes in the system dynamics resulting from the nonlinearities. Just as with the a_1 parameter, the c_1 and d parameters are relatively constant until the load change occurs. After the load change, d represents the change in the working steady state.

Transition from upper stable steady state to unstable steady state

In order to move the system to the unstable state, a sequence of small (10 degree) step changes in the set point was made. Figure 7 shows the temperature at $z = 0.206$ and the corresponding heat input for this run. All set point changes were followed very closely, with only the third set point change showing a slight overshoot. This figure illustrates the characteristic reversal of steady state gains between input and output as the system is moved from the upper stable state to the unstable state. For the first set point change, the controller must take out a slight amount of heat from the system to remain at the new set point; while for the last set point changes, the controller must put in more heat to remain at the new set point.

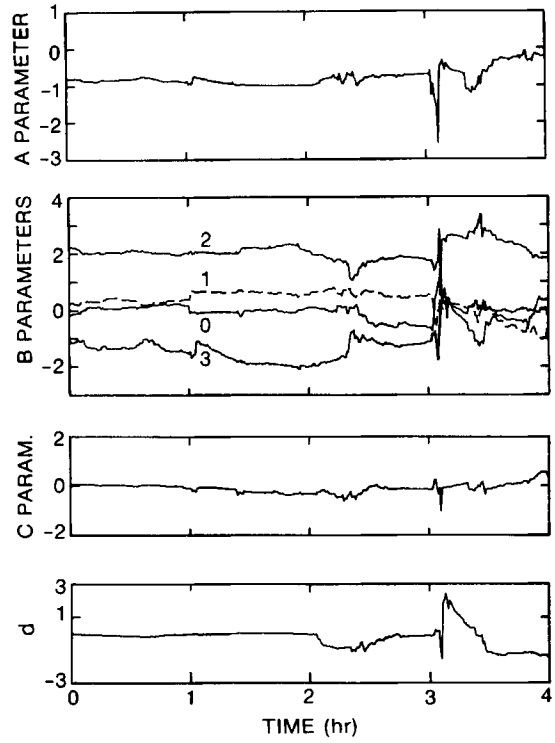

Figure 6. Model parameters for Fig. 4.

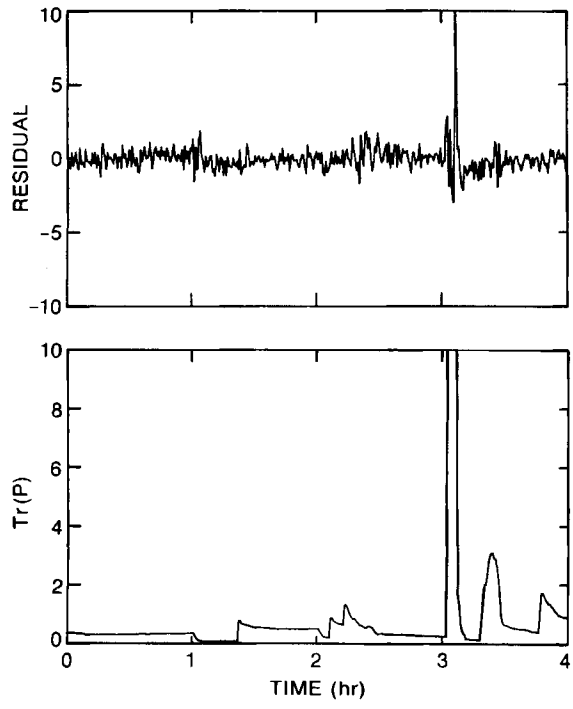

Figure 5. Residual sequence and trace of covariance matrix of Fig. 4.

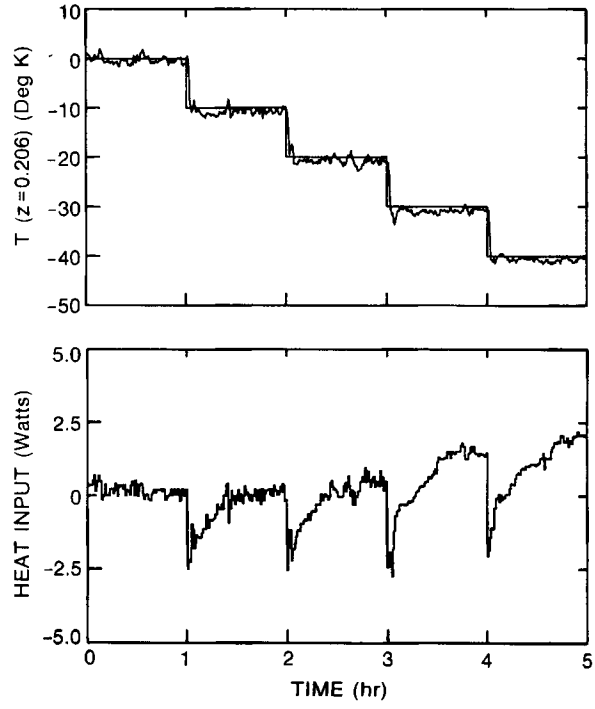

Figure 7. Transition from upper stable steady state to unstable steady state.

Figure 8 shows that the residual again exhibits small jumps at each set point change, similar to those shown in Figure 5. In this case, only the first set point change causes an increase in the elements of the covariance matrix, as indicated by the plot of its trace.

The behavior of the parameters is given in Figure 9. They all move around initially and after the first set point change because of the major increase in the elements of the covariance matrix (Figure 8). The first set point change forces the system drastically, yielding more information to the parameter estimator; consequently the parameters begin to converge to correct values. After the second set point change, all of the parameters have essentially converged. The changes in the parameters during each of the last three set point changes result from changes in process dynamics as the operating point is moved.

These changes in process dynamics as the reactor is moved from the upper stable steady state to the unstable steady state operating point are reflected in the changes in the closed-loop pole (Figure 10). In this case, the migration of the closed-loop pole toward the value of 1 during the course of this run indicates that the dynamics of the reactor are slowing down as it is driven from the upper stable steady state to the unstable steady state. This result is expected from a prior eigenvalue analysis of the dynamic reactor model (McDermott, 1984).

Control at the unstable steady state

The response of the reactor to step changes in the set point and in feed flow rate at the unstable state is shown in Figure 11. The reactor exhibits a large overshoot for the first set point change, at $t = 1$ h, again due to the extreme system nonlinearities, but soon settles out at the new set point. When the set point returns to the original value, the system shows little overshoot.

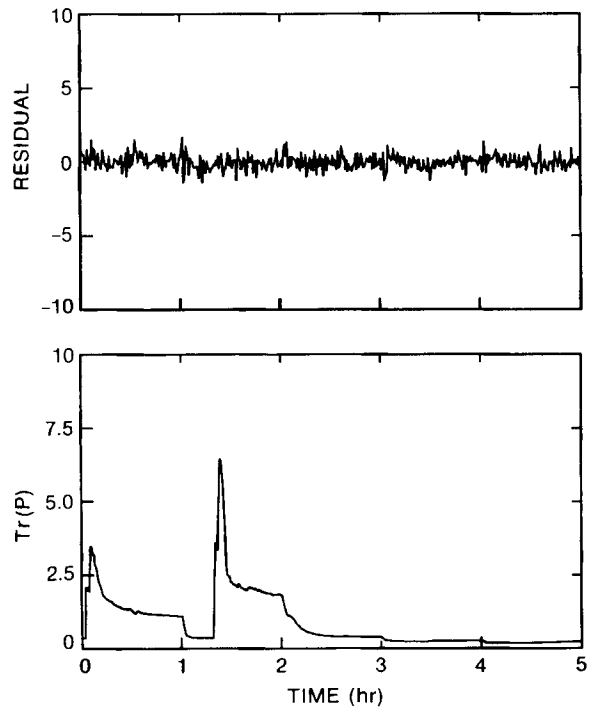

Figure 8. Residual sequence and trace of covariance matrix of Fig. 7.

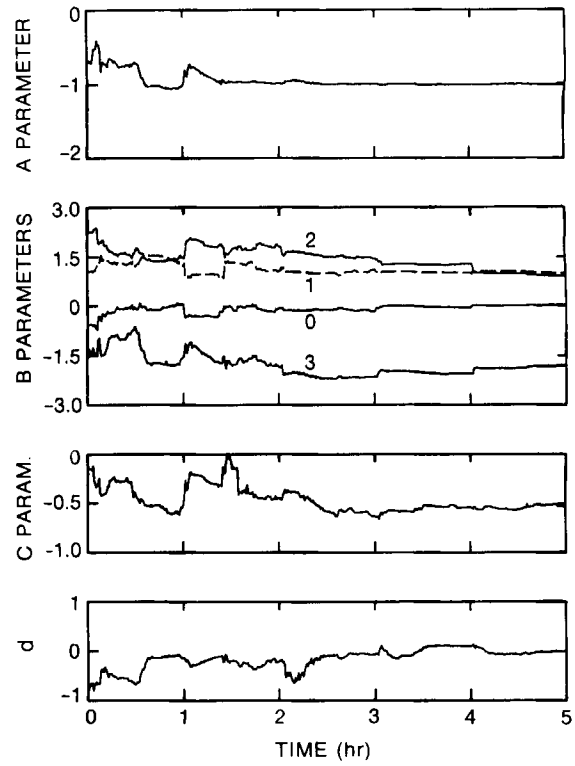

Figure 9. Model parameters for Fig. 7.

This behavior suggests that the system nonlinearities yield a stronger effect for set point changes in the positive direction.

The response of the reactor to a 20% decrease in the feed flow rate, at $t = 3$ h, shows that the controller performs very well for the load disturbance. The set point change after the load change is followed very closely, which illustrates how well the controller is able to retune itself after a major upset. However, the response of the reactor when the set point returns to the original value again exhibits a large overshoot, similar to the first set point change. This behavior confirms the earlier conjecture that the system nonlinearities are stronger for positive set point changes than for negative set point changes. Finally, at $t = 7$ h, the feed flow rate returns to the original value (i.e., before the 20% decrease) and the controller again handles the load disturbance well.

Figure 12 shows the behavior of the residual and the trace of the covariance matrix. There is a big jump in the residual for

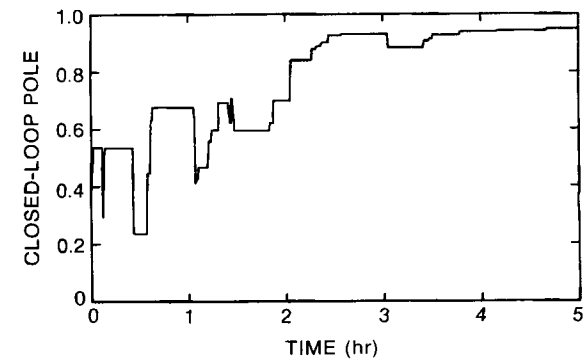

Figure 10. Closed-loop pole for Fig. 7.

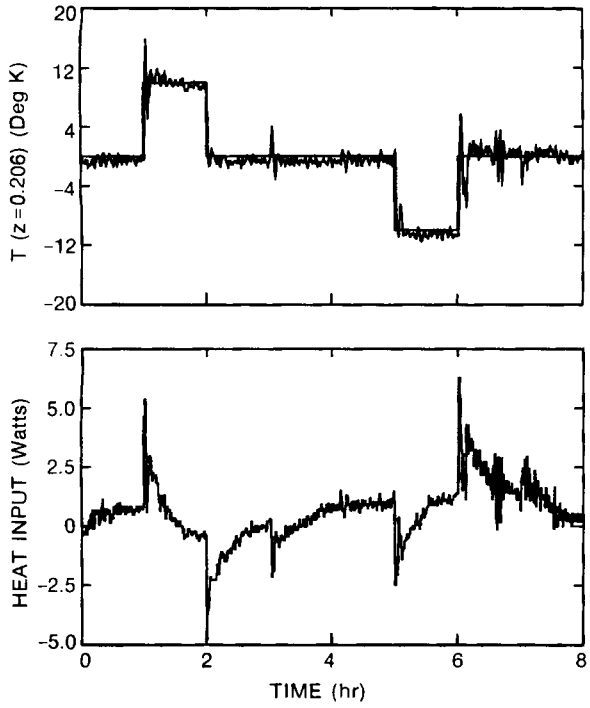

Figure 11. Response of reactor to set point and load (feed flow rate) step changes at unstable steady state, T_s = 40 s.

each positive set point change, indicating that the model was not able to accurately predict the behavior of the reactor for these changes. In contrast, there are only small jumps for negative set point changes. Large jumps in the residual also occur at each flow rate change, indicating immediately that an important modification of the system's operating conditions has occurred. The small jumps in the trace show that the fault-detection algorithm operates effectively, increasing the elements of the covariance matrix in order to force new parameter estimates whenever these are required. The jump in the residual at the first load disturbance (3 h) was not large enough to exceed the threshold. Hence, covariance resetting was not used at this time. Covariance resetting was reinitiated at the second positive set point change due to the large jump in the residual at this time.

Figure 13 gives the behavior of the model parameters. As was observed for the upper stable state, the parameters continually move about as operating conditions change.

The unstable state run was repeated with a new sampling period of 80 s (all other conditions remained constant). Figure 14 shows the response of the reactor to changes in the set point and load variable. In this case, all set points are followed closely and with very little overshoot. The amount of control action required initially for each set point change has been reduced by approximately one-third of that seen in the previous run; hence, the nonlinearities are not as strong for this run.

Figure 14 shows that the response of the system for the first load change is worse than the load response for the faster sampling period controller (Figure 11). The reason for this behavior is that the faster sampling period controller detected the change in the output due to the load disturbance sooner, and was able to take corrective action immediately. Since the slower sampling period controller took twice as long to notice the change in the output, the effect of the load disturbance was larger. This then caused the residual to exceed the threshold, Figure 15, and initiate covariance resetting. During this period, the controller output was filtered, thereby reducing the effectiveness of the controller disturbance rejection abilities.

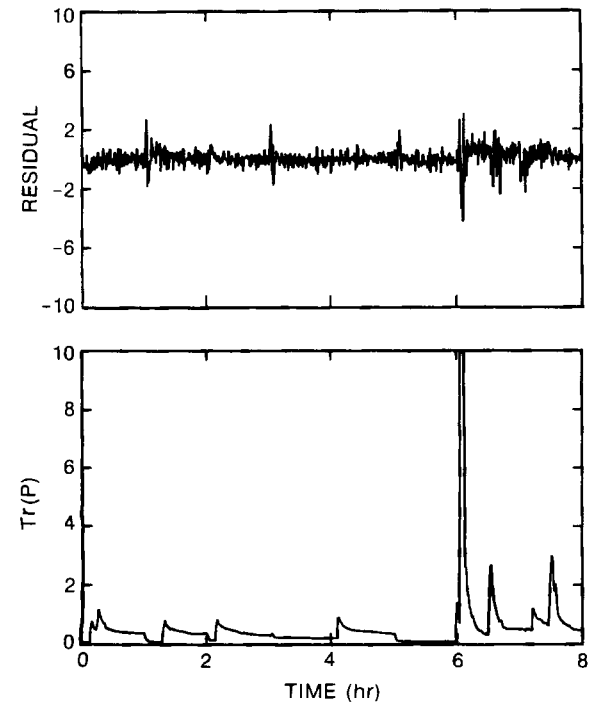

Figure 12. Residual sequence and trace of covariance matrix of Fig. 11.

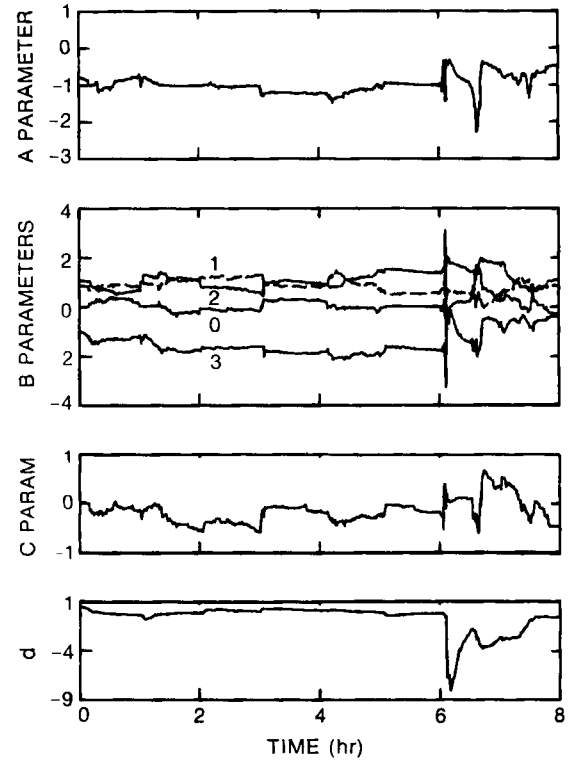

Figure 13. Model parameters for Fig. 11.

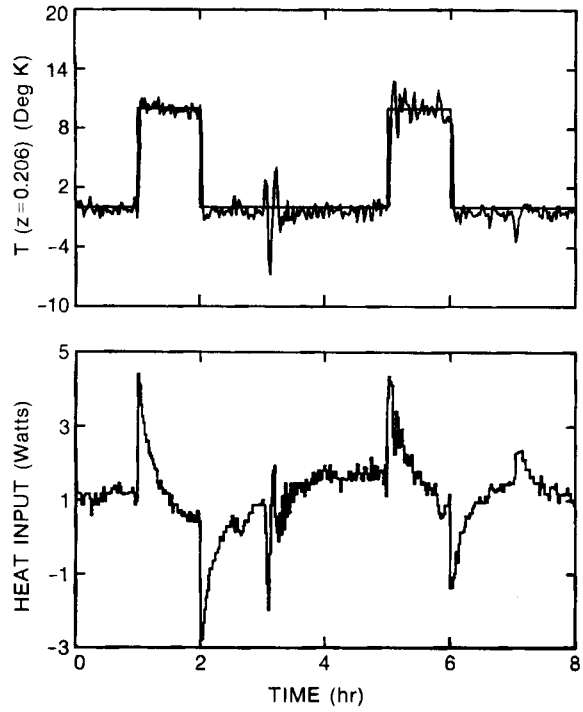

Figure 14. Response of reactor to set point and load (feed flow rate) step changes at unstable steady state, T_s = 80 s.

Figure 15 shows that there is a major jump in the residual for only the load change. There is a slight jump in the trace for the set point change after the load change, indicating that the parameters had not converged to the correct values. The parameter estimates are very well behaved for this run, as Figure 16 shows. The covariance resetting causes the big change at t = 3 h, while the second set point change produces the second jump. However, after both of these upsets, the parameters settle out very quickly.

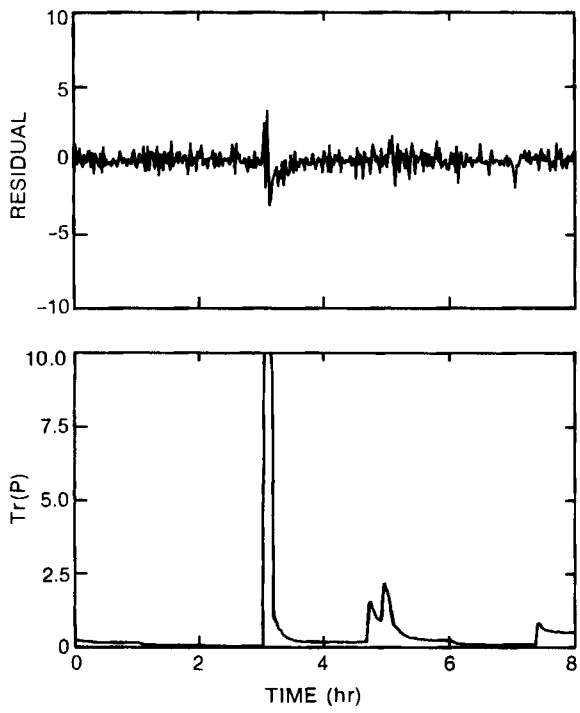

Figure 15. Residual sequence and trace of covariance matrix of Fig. 14.

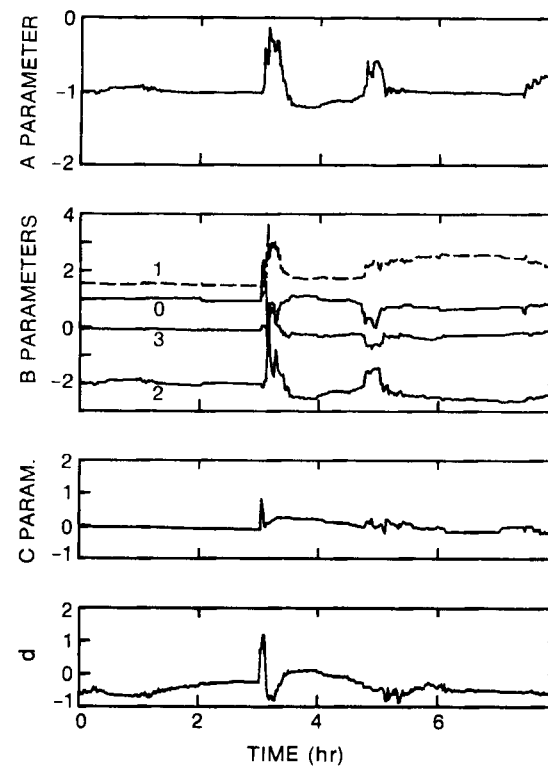

Figure 16. Model parameters for Fig. 14.

In this paper we have demonstrated the self-tuning control of a highly nonlinear fixed-bed reactor. Using a single-input/single-output control configuration, excellent set point tracking and disturbance rejection properties were obtained. In Part II, we consider the multivariable control of this reactor.

Acknowledgment

The support of this work under National Science Foundation Grant No. CPE 81-12668 is gratefully acknowledged.

Notation

$A(z^{-1})$, $B(z^{-1})$, $C(z^{-1})$ = process model polynomials of orders n_A, n_B, and n_c, respectively
d = offset term
$E(z^{-1})$, $E^{\dagger}(z^{-1})$, $F(z^{-1})$, $F^{\dagger}(z^{-1})$, $H(z^{-1})$ = general polynomials
I = objective function
$\underline{I}$ = identity matrix
k_{min} = minimum expected time delay
$\underline{P}$ = covariance matrix
$P(z^{-1})$, $Q(z^{-1})$, $R(z^{-1})$ = objective function weighting polynomials
R = reactor radius, m
R_c = inside radius of outer tube, m
R_i = outside radius of inner tube, m
R_{ins} = radial thickness of insulation, m
R_o = outside radius of outer tube, m
t = time in sampling instants (integer)
T = temperature, K
T_r = trace of covariance matrix
T_s = sampling time
$u(t)$ = system input at time t
$V(z^{-1})$ = desired closed-loop polynomial

v_1 = desired closed-loop pole
$y_r(t), y(t)$ = system set point and output, respectively, at time t
z^{-1} = backward shift operator, $z^{-1}u(t) = u(t-1)$
z = axial distance, dimensionless
$\gamma = E(1)d$
ξ = uncorrelated random sequence of zero mean
$\phi(t + k_{min})$ = generalized output

Literature Cited

Allidina, A. Y., and F. M. Hughes, "Generalized Minimum Variance Control with Pole Placement," *Proc. IEE*, **127,** Pt. D, 13 (1980).

Ampaya, J. P., and R. G. Rinker, "Autothermal Reactors with Internal Countercurrent Heat Exchange—Numerical and Experimental Studies in the Multiple Steady State Region," *Chem. Eng. Sci.*, **32,** 1,327 (1977).

———, "Autothermal Reactors with Internal Countercurrent Heat Exchange—Numerical and Preliminary Experimental Studies of Transient Behavior Including Start-up in the Multiple Steady State Region," *Chem. Eng. Sci.*, **33,** 703 (1978).

Åström, K. J., "Self-tuning Control of a Fixed-Bed Chemical Reactor System," Report TFRT-3151, Dept. Auto. Control, Lund Inst. Tech., Lund, Sweden, (Nov., 1978).

Åström, K. J., U. Borisson, and B. Wittenmark, "Theory and Applications of Self-tuning Regulators," *Automatica*, **13,** 457 (1977).

Åström, K. J., and B. Wittenmark, "Analysis of a Self-tuning Regulator for Nonminimum-Phase Systems," *Proc. IFAC Stochastic Control Symp.*, Budapest (1974).

———, "On Self-tuning Regulators," *Automatica*, **9,** 185 (1973).

———, "Self-tuning Controllers Based on Pole-Zero Assignment," *Proc. IEE*, **127,** Pt. D, 120 (1980).

Bonvin, D., R. G. Rinker, and D. A. Mellichamp, "On Controlling an Autothermal Reactor at an Unstable State. I: Steady State and Dynamic Modeling," *Chem. Eng. Sci.*, **38,** 233 (1983a).

———, "On Controlling an Autothermal Reactor at an Unstable State. II: Discrimination among Rival Models to Achieve Suitable Internal Structure," *Chem. Eng. Sci.*, **38,** 245 (1983b).

———, "On Controlling an Autothermal Reactor at an Unstable State. III: Model Reduction and Control Strategies which Avoid State Estimation," *Chem. Eng. Sci.*, **38,** 607 (1983c).

Clarke, D. W., and P. J. Gawthrop, "Self-tuning Controller," *Proc. IEE*, **122,** 929 (1975).

———, "Self-tuning Control," *Proc. IEE*, **126,** 633 (1979).

———, "Implementation and Application of Microprocessor-based Self-tuners," *Automatica*, **17,** 233 (1981).

Clement, K., S. B. Jørgensen, and J. P. Sørensen, "Fixed-bed Reactor Kalman Filtering and Optimal Control. II: Experimental Investigation of Discrete Time Case with Stochastic Disturbances," *Chem. Eng. Sci.*, **35,** 1,231 (1980).

Fortiscue, T. R., L. S. Kershenbaum, and B. E. Ydstie, "Implementation of Self-tuning Regulators with Variable Forgetting Factors," *Automatica*, **17,** 831 (1981).

Foss, A. S., J. M. Edmunds, and B. Kouvaritakis, "Multivariable Control System for Two-Bed Reactors by the Characteristic Locus Method," *Ind. Eng. Chem. Fundam.*, **19,** 109 (1980).

Hägglund, T., "Adaptive Control with Fault Detection," Report TFRT-7242, Dept. Auto. Control, Lund Inst. Tech., Lund, Sweden (1982).

Harris, T. J., J. F. MacGregor, and J. D. Wright, "Self-tuning and Adaptive Controllers: An Application to Catalytic Reactor Control," *Technometrics*, **22,** 153 (1980).

Hodgson, A. J. F., and D. W. Clarke, "Self-tuning Control Applied to Batch Reactors," *IEE Conf. Appl. Adaptive and Multivar. Control*, Hull, England, 146 (1982).

Jutan, A., J. F. MacGregor, and J. D. Wright, "Multivariable Stochastic Control of a Pilot-plant Packed-bed Tubular Reactor," *5th IFAC/IFIP Int. Conf. Digital Comp. Appl. to Process Control*, The Hague, Netherlands (1977a).

Jutan, A., et al., "Multivariable Computer Control of a Butane Hydrogenolysis Reactor. I: State-Space Reactor Modeling," *AIChE J.*, **23,** 732 (1977b).

Jutan, A., J. D. Wright, and J. F. MacGregor, "Multivariable Computer Control of a Butane Hydrogenolysis Reactor. II: Data Collection, Parameter Estimation, and Stochastic Disturbance Identification," *AIChE J.*, **23,** 742 (1977c).

———, "Multivariable Computer Control of a Butane Hydrogenolysis Reactor. III: On-line Linear Quadratic Stochastic Control," *AIChE J.*, **23,** 751 (1977d).

———, "Design and On-line Implementation of a Stochastic Controller Using an Identified Multivariable Noise Model," *Proc. Joint Auto. Control Conf.*, San Francisco (1980).

Kalman, R. E., "Design of a Self-optimizing Control System," *Trans. ASME*, **80,** Ser. D, 468 (1958).

Lee, R. W., "Dynamic Behavior of an Autothermal Reactor with Internal Countercurrent Heat Exchange," Ph.D. Diss., Univ. California, Santa Barbara (1978).

Lee, K. S., and W. K. Lee, "On-line Optimizing Control of a Nonadiabatic Fixed-bed Reactor," *AIChE J.*, **31,** 667 (1985).

McDermott, P. E., "Self-tuning Control of a Tubular Autothermal Reactor," Ph.D. Diss., Univ. California, Santa Barbara (1984).

McDermott, P. E., and D. A. Mellichamp, "An Auto-Pole-placement Self-tuning Controller," *Int. J. Cont.*, **40,** 1,131 (1984a).

McDermott, P. E., D. A. Mellichamp, and R. G. Rinker, "Multivariable Self-tuning Control of a Tubular Autothermal Reactor," *Proc. ACC.*, 1,616 (1984b).

Seborg, D. E., S. L. Shah, and T. F. Edgar, "Adaptive Control Strategies for Process Control: A Survey," AIChE Diamond Jubilee Meet., Washington, DC (1983).

Silva, J. M., P. H. Wallman, and A. S. Foss, "Multibed Catalytic Reactor Control Systems: Configuration Development and Experimental Testing," *Ind. Eng. Chem. Fundam.*, **18,** 383 (1979).

Sørensen, J. P., "Experimental Investigation of the Dynamics of a Fixed-bed Reactor," *Chem. Eng. Sci.*, **31,** 719 (1976).

———, "Experimental Investigation of the Optimal Control of a Fixed-bed Reactor," *Chem. Eng. Sci.*, **32,** 763 (1977).

Sørsensen, J. P., S. B. Jørgensen, and K. Clement, "Fixed-bed Reactor Kalman Filtering and Optimal Control. I: Computational Comparison of Discrete vs. Continuous Time Formulations," *Chem. Eng. Sci.*, **35,** 1,223 (1980).

Tremblay, J. P., and J. D. Wright, "Multivariable Model Reference Adaptive Control of a Pilot-Scale Packed-bed Tubular Reactor," *5th IFAC/IFIP Int. Conf. Digital Computer Appl. Process Control,"* The Hague, Netherlands (1977).

Vogel, E. F., "Adaptive Control of Chemical Processes with Variable Dead Time," Ph.D. Diss., Univ. Texas, Austin (1982).

Vogel, E. F., and T. F. Edgar, "Application of an Adaptive Pole-Zero Placement Controller to Chemical Processes with Variable Dead Time," *Proc. Am. Control Conf.*, Arlington, VA (1982).

Wallman, P. H., J. M. Silva, and A. S. Foss, "Multivariable Integral Controls for Fixed-bed Reactors," *Ind. Eng. Chem. Fundam.*, **18,** 392 (1979).

Wellstead, P. E., D. Prager, and P. Zanker, "Pole-assignment Self-tuning Regulator," *Proc. IEE*, **126,** 781 (1979a).

Wellstead, P. E., et al., "Self-tuning Pole-Zero Assignment Regulators," *Int. J. Control*, **30,** 1–26 (1979b).

Wellstead, P. E., and P. Zanker, "Servo Self-tuners," *Int. J. Control*, **30,** 27 (1979c).

Wellstead, P. E., and S. P. Sanoff, "Extended Self-tuning Algorithm," *Int. J. Control*, **34,** 433 (1981).

Wong, C., et al., "On Controlling an Autothermal Reactor at an Unstable State. IV: Model Fitting and Control of the Laboratory Reactor," *Chem. Eng. Sci.*, **38,** 619 (1983).

Wright, J. D., et al., "Inferential Control of an Exothermic Packed-bed Tubular Reactor," *Proc. Joint Auto. Control Conf.*, San Francisco (1977).

Manuscript received July 9, 1984, and revision received Oct. 24, 1985.